Evaluation of the Consistency of Long-Term NDVI Time Series Derived From AVHRR, SPOT-Vegetation, SeaWiFS, MODIS, and Landsat ETM+ Sensors

Molly E. Brown, Jorge E. Pinzón, Kamel Didan, Jeffrey T. Morisette, and Compton J. Tucker

***Abstract*—This paper evaluates the consistency of the Normalized Difference Vegetation Index (NDVI) records derived from Advanced Very High Resolution Radiometer (AVHRR), SPOT-Vegetation, SeaWiFS, Moderate Resolution Imaging Spectroradiometer, and Landsat ETM+. We used independently derived NDVI from atmospherically corrected ETM+ data at 13 Earth Observation System Land Validation core sites, eight locations of drought, and globally aggregated one-degree data from the four coarse resolution sensors to assess the NDVI records agreement. The objectives of this paper are to: 1) compare the absolute and relative differences of the vegetation signal across these sensors from a user perspective, and, to a lesser degree, 2) evaluate the possibility of merging the AVHRR historical data record with that of the more modern sensors in order to provide historical perspective on current vegetation activities. The statistical and correlation analyses demonstrate that due to the similarity in their overall variance, it is not necessary to choose between the longer time series of AVHRR and the higher quality of the more modern sensors. The long-term AVHRR-NDVI record provides a critical historical perspective on vegetation activities necessary for global change research and, thus, should be the basis of an intercalibrated, sensor-independent NDVI data record. This paper suggests that continuity is achievable given the similarity between these datasets.**

***Index Terms*—Advanced Very High Resolution Radiometer (AVHRR), Moderate Resolution Imaging Spectroradiometer (MODIS), SPOT, vegetation.**

I. Introduction

VARIOUS remote-sensing-based studies have revealed compelling spectral relationships between the red and near-infrared (NIR) part of the spectrum to green vegetation [1]. Due to vegetation pigment absorption (chlorophyll, proto-chlorophyll), the reflected red energy decreases, while the reflected NIR energy increases as a result of the strong scattering processes of healthy leaves within the canopy. Directly using the amount of reflected red and/or NIR radiation to study the biophysical characteristics of vegetation is very inadequate, for reasons rooted in the intricate radiative energy interaction at the canopy level, background, and atmospheric impacts on the signal and the nonuniqueness of the signatures. When, however, two or more bands are combined into vegetation index (VI), the vegetation signal is boosted and the information become more useful [2]. Vegetation indices can then be used as surrogate measures of vegetation activity [3], [4]. The most widely used form of VI, the Normalized Difference Vegetation Index (NDVI), was introduced by Deering in 1978 [5] and Tucker in 1979 [3] and is the ratio of the difference of the NIR and red band divided by their sum. The NDVIs properties help mitigate a large part of the variations that result from the overall remote-sensing system (radiometric, spectral, calibration, noise, viewing geometry, and changing atmospheric conditions). Some land-surface types are not robustly represented by NDVI, such as snow, ice, and nonvegetated surfaces, where atmospheric variations and sensor characteristics dominate [6].

NDVI is often used as a monitoring tool for the vegetation health and dynamics, enabling easy temporal and spatial comparisons [7]. In order to make effective use of NDVI data, issues related to the remote-sensing system need to be addressed. The most serious are clouds, which render any observation useless by obstructing the target, and, to a lesser degree, the effects of the Bidirectional Reflectance Distribution Function (BRDF). To overcome these issues, maximum value compositing was developed as an operational approach to producing cloud free consistent NDVI maps. Multiple daily images are processed to create a representative, cloud-free image with the least atmospheric attenuation and viewing geometry effects [8]. The maximum value compositing (MVC) technique is the most widely used method and is based on maximizing the NDVI signal over a preset period of time. While MVC helps screen for clouds, it was found to also favor extreme viewing geometry (large solar zenith angles and large view angles in the forward scatter direction) [9] and, to a lesser extent, cloud shadow. Several studies attempted to address these issues with modest and mixed results [10]–[12].

On a global basis, several factors can influence differences in NDVI across sensors. Impacts from BRDF are well documented [10], [13]. Additionally, the Spectral Response Functions (SRFs) for the different sensors can lead to systematic differences in NDVI [14]. Each sensor has its own instantaneous field of view, swath width, and orbiting geometry. Ad-

Manuscript received November 1, 2004; revised August 12, 2005. This work was supported in part by USAID's Famine Early Warning System Network.

M. E. Brown and J. E. Pinzón are with the SSAI/NASA Goddard Space Flight Center, Greenbelt, MD 20771 USA (e-mail: molly.brown@gsfc.nasa.gov).

J. T. Morisette and C. J. Tucker are with the NASA Goddard Space Flight Center, Greenbelt, MD 20771 USA.

K. Didan is with the TBRS Laboratory, Soil, Water and Environmental Sciences, University of Arizona, Tucson, AZ 85721 USA.

Digital Object Identifier 10.1109/TGRS.2005.860205

justing for this list of known differences is somewhat tractable but, in many cases, beyond the capability or resources available to many users [15]. In this study, we evaluate the publicly available NDVI products from four operational NDVI products from four sensors. Our analysis is conducted without any adjustment for BRDF or sensor-specific characteristics (such as SRF). The justification for this approach is to conduct a user-based analysis to indicate by how much and where these operational products differ.

In the context of NASA's Committee on Earth Observation Satellites (EOS), validation is defined as "the process of assessing by independent means the quality of the data products derived from the system outputs" [16]. In this paper, we first utilize NDVI from ETM+ data as the independent data by which we assess the quality of NDVI output from Advanced Very High Resolution Radiometer (AVHRR), SPOT-VGT, SeaWiFS, and MODIS. The definition allows for intercomparisons between sensors to assess the general agreement of the output from these sensors, as long as that output is independently constructed. For our sensor intercomparison, we examine eight areas where droughts were detected between 2000 and 2004, 13 EOS validation sites, as well the global distribution in difference between the four sensors. The goal of this paper is provide the user of operationally available NDVI products an understanding of how to properly interpret and utilize these data and suggest applications where further adjustments to the operational products would be required for analysis involving data from multiple sensors.

II. Data and Methods

Data from four sensors were used in this study: global products from AVHRR on the NOAA satellites, SPOT Vegetation (VGT), land data from SeaWiFS and MODIS NDVI products. In addition, high resolution NDVI data from Landsat 7's Enhanced Thematic Mapper plus (ETM+) were used as an independent measure (Table I).

TABLE I
NDVI Datasets Used in This Study: Sensors and the Data Source, Spatial and Temporal Resolutions, Equatorial Crossing Time, and Field of View for Each Sensor

Sensor	AVHRR	SPOT Vegetation	MODIS	SeaWiFS	LandSAT ETM+
Data Source	GIMMS NDVIg Operational Dataset	FAS-GIMMS, VITO	MODIS-Land and Vermote/ Saleous	SeaWiFS/ GSFC/GIMMS	Corrected scenes from EOS web
Spatial Resolution	8000 m and 1 degree	1000 m and 1 degree	500 m, 5000 m, 1degree	4633 m, 1 degree	30 m
Temporal Resolution	15 day and monthly	10 day and monthly	16-day and monthly	monthly	1 to 9 scenes, 1999-2001
Equatorial Crossing	~9 AM - ~6 PM	10.30 AM	10.30 AM	12.05 PM	10:00 AM
Field of View (FOV)	±55.4°	±101°	±55°	±58.3°	±15.4°

A. Data

All four NDVI time series are based on the maximum value compositing technique [8]. This method minimizes differences in the spectral properties, radiometric resolution, residual atmosphere effects, and, most importantly, minimizes clouds. By selecting the pixel with the maximum NDVI signal and minimum atmospheric effects, the same day is usually selected for each sensor reducing any temporal discrepancies in the time series. In the case of MODIS sensor, a constrained-view MVC (CV-MVC) is used to minimize the off-nadir tendencies of the MVC.

We used maximum-value AVHRR NDVI composites [8] from the NASA Global Inventory Monitoring and Modeling Systems (GIMMS) group at the Laboratory for Terrestrial Physics [18] from July 1981–May 2004. A postprocessing satellite drift correction has been applied to this dataset to further remove artifacts due to orbital drift and changes in the sun-target-sensor geometry [19]. As a result of AVHRR's wide spectral bands, it is more sensitive to water vapor in the atmosphere. An increase in water vapor results in a lower NDVI signal, which can be interpreted as an actual change if no correction is applied [20]. The maximum value composite should lessen these artifacts. The GIMMS operational dataset incorporates data from sensors aboard NOAA-7 through 14 with the data from the AVHRR on NOAA-16 and 17 using SPOT data as a bridge for a by-pixel intercalibration. Details of these corrections can be found in [18] and [19]. After calibration, the AVHRR NDVI data dynamic range was adjusted to values of -0.05 to 0.95 to match more closely that of the SPOT- and MODIS-based NDVI.

The SPOT VGT data used in this study are VGT-S10 (ten-day synthesis) products. The "S10-composited" data (spectral band data, data quality and NDVI) covering the period May 1998–June 2004 were acquired for analysis. Postprocessing includes reprojection from the native global Mercator to a continental Albers projection, regional subsetting, cloud screening, and land masking.

The MODIS 16-day 500-m (MOD13A1) data [21] is available in the sinusoidal projection over spatial units called tiles that are $10^\circ \times 10^\circ$ ($\sim 1200 \times 1200$) km. This data was stitched and reprojected to the Albers Equal Area to match the AVHRR product [22]. In addition to the standard 16-day MODIS NDVI, a 0.05° (5.6 km) monthly climate modeling grid (MOD13C2) product was also used. This data will soon be available to the public via the EDC-DAAC and will provide an opportunity for direct comparison with the SPOT, SeaWiFS, and AVHRR products. Data from February 2000–August 2004.

The fourth global NDVI dataset is from SeaWiFS. Channels 6 and 8 were atmospherically corrected for Rayleigh scattering and oxygen absorption and then composited into monthly images [8]. The data, in the sinusoidal grid at 4.63-km resolution, covers the period September 1997–October 2002 for all continents except Antarctica. A provisional one-degree aggregated monthly product was also used in this study as an additional source of comparison.

Finally, atmospherically corrected surface reflectances from Landsat ETM+ level 1G subsets at 30-m resolution were used to create an ETM+ NDVI data set [23]. The atmospheric correction used the 6S radiative transfer code [24]. The input parameters needed by 6S to correct the ETM+ scenes were water vapor, aerosol optical depth, and total ozone, other parameters were preset in the 6S code for ETM+. Each ETM+ scene was centered on an Aerosol Robotic Network (AERONET) location [25] site, which provides water vapor and aerosol optical depth measurements. These NDVI images were first subset to match the 25×25 km area for each site, and then all pixels in the

subset averaged to create one data point per time period. The NDVI standard deviations in the ETM+ subset were calculated to provide a measure of heterogeneity in the scene [17]. The ETM+ data covers the period 1999–2001 (Table I).

B. Methods

To compare the interannual NDVI signal, we have selected windows of 25 × 25 km and one degree, with a monthly temporal sampling that provide the least common denominator amongst the datasets. The spatial resolution impact on NDVI will not be addressed here, as it was addressed by various multiscale analyses [26]. We will, however, focus on the spectrally induced differences in the datasets using statistical and empirical methods. Differences in the temporal resolution, or composite period, between the different datasets are less important here and are somewhat moderated by the overall length of the time series record. Since only the AVHRR dataset is of sufficient length to capture trends at the decadal scale, we will, therefore, focus on the interannual variability captured by the shorter of the records in this study.

The average of all pixels in a 25 × 25 km window, centered on the study sites (Table II), is used to compare the NDVI time series. This footprint is commonly used to evaluate local vegetation dynamics and allows for the use of the AVHRR dataset with the lowest spatial resolution. In 8000-m data, this means that nine pixels are averaged to create the NDVI value for each time period. The time series was used to provide a statistical description of each site and sensor with a mean and standard deviation from all months from each site.

In addition, all datasets were aggregated to one degree and monthly time step, the spatial and temporal resolution that is most frequently used by climate and other biophysical modelers [27], [28]. This coarse resolution provides the ability to examine the range of land cover types, from arctic tundra to humid tropical forest, and is a commonly used spatial resolution in biophysical and climate modeling studies [29].

The datasets were first compared at the sensor's native temporal resolution (ten-day, 15-day, 16-day, and monthly), and then re-examined at the standardized monthly time step. Because each dataset in this analysis has a different temporal compositing period, the datasets were aggregated to a monthly time step using the NDVI maximum-value compositing method [8]. This provides a common temporal scale, as well as enabling the direct comparisons of the time series.

We used the Landsat ETM+ data as validation for the study. Atmospherically corrected Landsat ETM+ NDVI data over EOS land validation core sites are independent and of high-enough resolution to provide detailed and accurate representation of the ground vegetation and, hence, can be an alternative validation surrogate in this study.

TABLE II
NAME, LAND COVER, AND LOCATION CHARACTERISTICS OF THE STUDY SITES USED IN THIS PAPER IN ALPHABETICAL ORDER. THE EOS SITES ARE MARKED WITH AN ASTERISK (*)

	Latitude	Longitude	Closest City, State, Country	Annual Precip. (mm)	Min temp (°C)	Max temp (°C)
Barrow *	71.32	-156.69	Barrow, Alaska, USA	116	4.5	15.3
Bondville *	40.06	-88.39	Bondville, Illinois, USA	981	5.3	16.2
Cascades *	44.25	-122.25	Springfield, Illinois, USA	1180	5.3	17.4
Crystal City	28.69	-99.86	Crystal City, Texas, USA	545	15.9	28.5
E.Longreach	-23.00	145.50	Longreach, Queensland, Australia	497	15.0	30.6
Gujarat	22.00	70.00	Rajkot, Gujarat,India	576	20.5	32.4
Harvard *	42.53	-72.20	Amherst, Massachusetts, USA	1062	1.8	14.7
Ji-Parana *	-10.75	-62.37	Ji-Parana, Rondonia,Brazil	1813	20.1	31.3
Konza *	39.11	-96.63	Manhattan, Kansas, USA	884	6.0	18.7
Louga	16.00	-16.00	Ndinbou, Louga,Senegal	257	19.8	34.4
Lyon	46.00	5.00	Villars-les-Dombes Rhone, France	861	6.3	15.0
Mongu *	-15.25	23.16	Kataba, Mongu, Zambia	906	15.5	29.9
Parkfall	45.93	-90.28	Park Falls, Wisconsin, USA	784	-0.6	10.1
Rajasthan	26.00	74.50	Ajmer, Rajasthan, India	574	18.5	32.1
Saskatchewan	50.00	-110.00	Walsh, Alberta, Canada	323	-2.6	11.1
Sevilleta *	34.36	-106.91	Veguita, New Mexico, USA	342	0.4	19.8
Skukuza *	-24.99	31.59	Skukuza, Transvaal, South Africa	557	15.3	29.2
Sydney	-31.14	150.75	Tamworth, New South Wales, Australia	715	10.2	23.5
Tapajos *	-2.42	-54.77	Santarem, Para, Brazil	1524	24.0	27.1
USDA-BARC	39.03	-76.89	Greenbelt, Maryland, USA	1065	6.8	18.3
Walker *	35.96	-84.31	Oak Ridge, Tennessee, USA	1342	6.6	19.4

III. RESULTS

The AVHRR NDVI dataset provides a bridge between the historical record and the modern satellites allowing an extension of their relatively short records, assisting global change researchers who use vegetation data [30], [31]. Fig. 1 shows the time series from AVHRR, SPOT-VGT, and two MODIS datasets for the Bondville, IL, site [32]. This plot shows that all four sensors are able to capture the annual green-up and brown-down of the vegetation to a similar degree. The similarity of the series is very encouraging and is driving plans to connect the much longer AVHRR record to the other sensors, and, eventually, to the Visible/Infrared Imager/Radiometer Suite (VIIRS) sensors aboard the National Polar-Orbiting Operational Environmental Satellite System (NPOESS) Preparatory Project (NPP). Data continuity in the vegetation record is central to scientists' ability to measure the impact of global environmental change on terrestrial ecosystems.

The peaks in NDVI shown in Fig. 1 occur at approximately the same time during the four years of overlap. Differences in the exact start and end of the growing season are to be expected with differences in the compositing period for data shown (monthly, 16-day, 15-day, and 10-day maximum value composites). Variations in these records due to the mechanics of NDVI and maximum value compositing (MVC) should affect all these NDVI

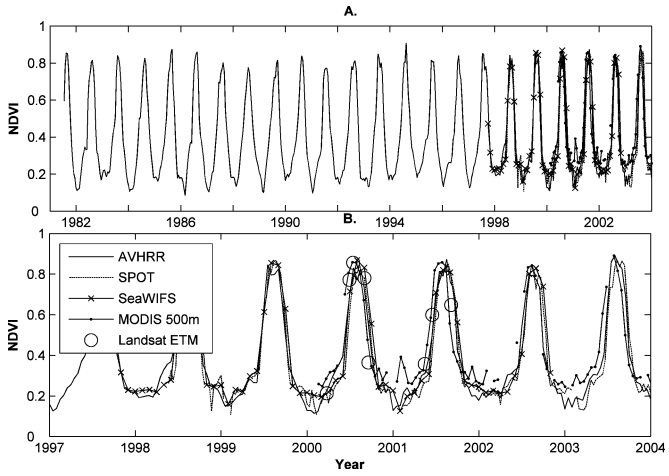

Fig. 1. NDVI temporal profiles for the Bondville, IL, site. Fifteen-day AVHRR, ten-day SPOT VGT, 16-day MODIS 500 m, monthly lat-lon MODIS 5.6 km, and monthly SeaWiFS data are plotted. The Landsat NDVI averages are also plotted (circles). All data represent the average NDVI for a 25 × 25 km window. Top panel shows the AVHRR 1981–2003 record and the bottom hightlights the 1997–2004 period of the same series.

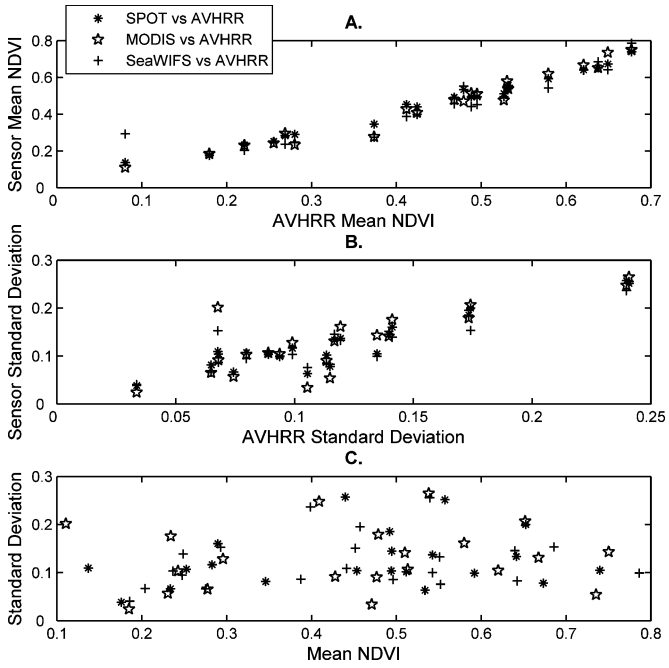

Fig. 2. Scatter plot of the mean time series data for SPOT, MODIS, and SeaWiFS NDVI versus AVHRR NDVI for all sites in Table II. (A) Mean NDVI from time series data. (B) Standard deviation from time series data. (C) Mean NDVI versus standard deviations.

records equally. Large differences in the way snow and ice are treated between the five sensors can be seen during the winter months (December–February for this site). For comparison, the averaged Landsat ETM+ NDVI values for the site are plotted [33].

A. Intercomparison of NDVI Time Series

The results of the intercomparisons of the NDVI time series are presented in Fig. 2. This plot shows the relationship between the NDVI time series for all sensors by averaging all common periods and plotting these averages against each other. The more similar the series are to each other, the closer they will be to the one-to-one line [Fig. 2(a)]. The standard deviations of the time series from the four sensors are not as closely related, as the impact of clouds and aerosols on the time series creates variability that is influenced by the processing and spectral characteristics of the different sensors. AVHRR, in particular, is very sensitive to water vapor in the atmosphere, largely due to both AVHRR's radiometric characteristics (wider spectral bands more sensitive to atmospheric water vapor) and the perpetual presence of clouds in regions such as the Tapajos site, which are screened differently by the various algorithms [Fig. 2(b)]. Fig. 2(c) shows a fairly stable standard deviation across a variety of land cover types, as measured by the mean NDVI.

TABLE III
RMSE AND CORRELATION COEFFICIENT FOR THE AVHRR VERSUS OTHER SENSORS. CORRELATION WAS BASED ON ALL AVAILABLE MONTHLY DATA. THE NUMBER OF MONTHS IS REPORTED IN THE HEADER (i.e., $n = 67$). RMSE USES NDVI UNITS (0–1)

	RMSE			r^2		
	AVHRR-SPOT (n=67)	***AVHRR-MODIS*** (n=52)	***AVHRR-SeaWiFS*** (n=62)	***AVHRR-SPOT*** (n=67)	***AVHRR-MODIS*** (n=52)	***AVHRR-SeaWiFS*** (n=62)
Barrow	0.051	0.141	0.202	0.64	0.74	0.73
Bondville	0.040	0.078	0.063	0.97	0.90	0.94
Cascades	0.109	0.115	0.141	0.59	0.65	0.59
Crystal City	0.070	0.057	0.066	0.62	0.54	0.51
E.Longreach	0.073	0.131	0.141	0.52	0.52	0.32
Gujarat	0.043	0.062	0.061	0.89	0.84	0.87
Harvard	0.071	0.086	0.071	0.89	0.85	0.86
Ji-Parana	0.071	0.121	0.090	0.60	0.34	0.38
Konza	0.037	0.065	0.052	0.96	0.87	0.93
Louga	0.028	0.027	0.045	0.82	0.81	0.73
Lyon	0.039	0.097	0.064	0.85	0.27	0.85
Mongu	0.041	0.054	0.078	0.85	0.82	0.66
Parkfall	0.074	0.110	0.066	0.92	0.83	0.94
Rajasthan	0.050	0.053	0.049	0.79	0.76	0.84
Saskatchewan	0.062	0.119	0.091	0.94	0.92	0.88
Sevilleta	0.027	0.024	0.023	0.69	0.49	0.73
Skukuza	0.056	0.057	0.065	0.86	0.85	0.90
Sydney	0.076	0.071	0.077	0.90	0.91	0.92
Tapajos	0.098	0.106	0.103	0.04	0.02	0.39
USDA-BARC	0.047	0.091	0.042	0.89	0.77	0.91
Walker	0.049	0.057	0.057	0.88	0.90	0.89

Root mean-square error (RMSE) and linear correlations analyses of the monthly SPOT VGT, SeaWiFS and MODIS time series with the AVHRR dataset are presented in Table III. By presenting both the RMSE and the r^2, we are showing both the absolute difference between datasets, affected by the differences in the overall NDVI range, and the relative differences. The highest RMSE values were between MODIS and AVHRR due to the higher maximum NDVI values of the MODIS data, which is a direct result of its more sensitive red and NIR bands. The correlation and RMSE between NDVI from AVHRR and from the other sensors are presented in Table III. The correlation shows considerable similarity between the datasets, with the exception of the data from the Tapajos, reflecting the very strong influence of the atmosphere and the differences in atmospheric corrections over a tropical forest canopy.

A scatter plot of ETM+ NDVI and the NDVI data from the nearest composite period from the other sensors is shown in Fig. 3(a). ETM+ values provide a point estimate for a specific site on a specific date that has been atmospherically corrected using locally obtained observations, and thus provide a reference value to which the other sensor's NDVI can be compared. The NDVI values from SPOT, AVHRR and the 16-day MODIS data fell within plus/minus one standard deviation of the averaged ETM+ values, with the exception of the Mongu site

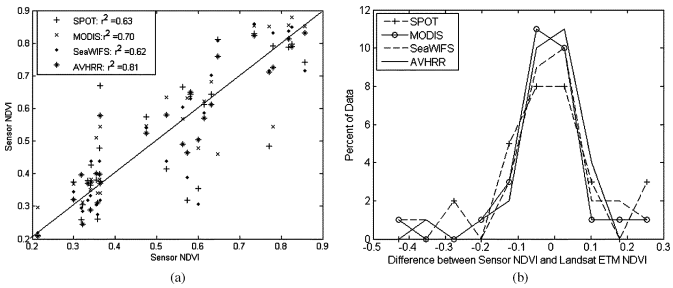

Fig. 3. Comparison of composited NDVI data to 22 Landsat ETM+ scenes. (a) Scatter plot of Landsat ETM+ NDVI (x axis) versus sensor NDVI (y axis) from the nearest maximum value composite to Landsat acquisition date. (b) Histogram of the NDVI difference between ETM+ and all other sensors given in NDVI units.

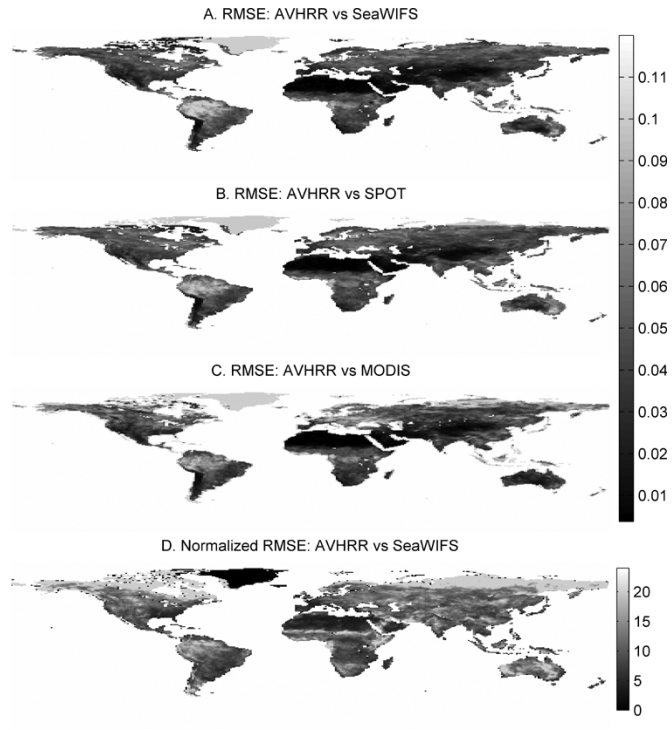

Fig. 4. Spatial distribution of the RMSE of the one-degree monthly aggregate NDVI anomalies of AVHRR subtracted from the anomalies of SeaWiFS, SPOT VGT, and MODIS. Panels A–C show the RMSE given in NDVI units. Panel D is the RMSE normalized by the average NDVI for AVHRR versus SeaWiFS, given in percent of NDVI units.

where the MODIS data fell within 1.07 standard deviations. Histograms of the difference between the Landsat ETM+ data and other sensors' NDVI are mostly centered around zero [Fig. 3(b)].

The results of these analyses show that, although the NDVI time series appear fairly comparable across sensors, closer inspection suggests that the data sets cannot be unconditionally interchanged with AVHRR. There are land cover-dependent differences, such as the tropical forests and high northern latitude tundra with large absolute differences ($>20\%$) between the datasets. These differences can either be related to the NDVI scaling, the interannual variability between the datasets, the different spectral characteristics, or a combined effect of all of them. We are interested in determining the similarity of these datasets, despite these factors, in the context of global vegetation change research.

B. Global Intercomparison

Regions where the datasets depart the most can more suitably be presented on global maps of RMSE of the one-degree NDVI anomalies datasets (Fig. 4). Moist tropical forests have the highest RMSE, with the largest differences observed in the Amazon basin. Deserts and regions with strong seasonality had low RMSE, below 0.05 NDVI units [Fig. 4(a)–(c)]. Some semiarid regions such as the Queensland province in Australia and the Kenyan rangelands showed higher RMSE. In general, however, users could confidently employ NDVI anomalies from all four datasets outside of the highly forested tropics as the differences between them were less than 0.1 NDVI units.

To identify specific regions where the NDVI anomalies were low, Fig. 4(d) shows the RMSE normalized from the mean SeaWiFS NDVI in percent NDVI units. This normalized RMSE is highest in the northern latitudes (above 65° north), where the different treatment of high solar zenith angles and snow and ice impact the NDVI signal. Regions where spatial resolution is important, such as in the Sahel in sub-Saharan Africa, results in anomalies at the one-degree level [34]. Relatively large differences in the NDVI from AVHRR and SeaWiFS are also seen in Australia where strong background signal and sparse vegetation tends to exaggerate spectral and atmospheric correction differences between the two datasets [35]. These RMSE maps show a low variability in the NDVI anomaly of less than 0.05 units for most areas.

The global maps showed that the northern latitudes had the largest absolute differences between the sensors. In general, vegetation indices are very unstable over snow/ice due to the bright nature of these targets and the mixing of snow/ice. These surfaces tend to generate very different surface reflectance values as a result of the calibration, correction, radiometric, spatial, and signal-to-noise characteristics of the sensor. These differences largely disappear and decline to only 10% of the signal when only the summer months were considered.

The similarity between the RMSE from the different datasets is investigated further in Fig. 5. These figures show the difference between the anomalies for all times and all places at one degree. We present three different time periods, as this analysis is sensitive to the overall climate conditions of the period of record. Notice in Fig. 5(c) that the solid line AVHRR histogram with the longest record has the mean that is closest to zero of all anomaly records, reflecting the much larger sample of climatic events. 85% of the overall difference fell within 0.150 NDVI units.

The variance structure of the datasets is similar, especially between SeaWiFS, SPOT and AVHRR. MODIS has a slightly higher zero anomaly-peak than AVHRR and SPOT. SPOT data has a more negative anomaly than the AVHRR or MODIS, with a mean of -0.005 NDVI. This is likely due to a poorer cloud screening that may have resulted from the lack of a thermal channel in SPOT, depressing the NDVI resulting in a slightly lower global anomaly [36]. The standard deviation of the global one-degree anomalies varied by land cover type, being lower in

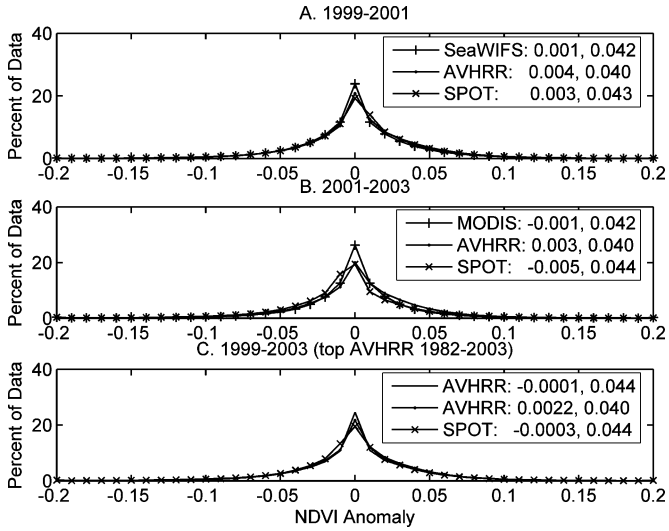

Fig. 5. Histograms of the one-degree anomalies. (A) Histograms of SeaWiFS, AVHRR and SPOT anomaly for 1999–2001. Mean and standard deviations of the global anomaly during that same period are shown on legend. (B) Histograms of MODIS, AVHRR, and SPOT anomaly for 2001 to 2003, with mean and standard deviations. (C) Histograms of AVHRR data for 1982–2003 (solid line) and SPOT and AVHRR for 1999–2003.

arid regions that have a smaller NDVI range, and larger in the tropical forests where NDVI is highest.

IV. Discussion and Conclusion

For the past decade, newer and more sophisticated sensors are becoming operational providing biophysical measurements that are aimed at addressing various global change related questions. NASA's MODIS sensors on-board Terra and Aqua satellites are providing a series of advanced remote-sensing-based land products [22], [37]. However, to achieve any meaningful monitoring of the land surface vegetation, stable, intercalibrated long term vegetation records (a decade or longer) are a key requirement [38]. Efforts for using data from MODIS and other sensors with the historic AVHRR vegetation NDVI records are proving to be challenging. There is a need for additional research into improving the long-term AVHRR data record and addressing the cross-sensor NDVI continuity [39].

Using the standard products instead of modeled simulations, we were able to intercompare various datasets with the historic AVHRR NDVI record. This analysis revealed that, although relatively large differences existed between the four NDVI datasets, the NDVI anomalies exhibited similar variances. Composited NDVI images are fairly robust, which can be seen when comparing time series with NDVI from Landsat ETM+ images that have been corrected for atmospheric effects.

This research suggests that progress can be made toward a unified NDVI dataset given that absolute variances across sensors are relatively similar, especially when seasonality is removed. Benefits of this work include enabling the use of the longer AVHRR time series to calculate the normal trends and any anomalies in combination with other sensors, the successful merging of various data sets from SPOT-VEG, MODIS, and SeaWiFS, and others quantitatively with the historic 25-year AVHRR NDVI data record, and the potential associated with using multiple NDVI data sources, especially in the event of one dataset's absence.

References

[1] J. E. Colwell, "Vegetation canopy reflectance," *Remote Sens. Environ.*, vol. 3, pp. 175–183, 1974.

[2] C. F. Jordan, "Derivation of leaf area index from quality of light on the forest floor," *Ecology*, vol. 50, pp. 663–666, 1969.

[3] C. J. Tucker, "Red and photographic infrared linear combinations for monitoring vegetation," *Remote Sens. Environ.*, vol. 8, pp. 127–150, 1979.

[4] C. J. Tucker, C. L. Vanpraet, M. J. Sharman, and G. van Ittersum, "Satellite remote sensing of total herbaceous biomass production in the Senegalese Sahel: 1980–1984," *Remote Sens. Environ.*, vol. 17, pp. 233–249, 1985.

[5] D. W. Deering, *Rangeland Reflectance Characteristics Measured by Aircraft and Spacecraft Sensors*. College Station, TX: Texas A&M Univ. Press, 1978, p. 338.

[6] R. Suzuki, T. Nomaki, and T. Yasunari, "Spatial distribution and its seasonality of satellite-derived vegetation index (NDVI) and climate in Siberia," *Int. J. Climatol.*, vol. 21, pp. 1321–1335, 2001.

[7] R. B. Myneni, C. D. Keeling, C. J. Tucker, G. Asrar, and R. R. Nemani, "Increased plant growth in the northern high latitudes from 1981 to 1991," *Nature*, vol. 386, pp. 698–702, 1997.

[8] B. Holben, "Characteristics of maximum-value composite images from temporal AVHRR data," *Int. J. Remote Sens.*, vol. 7, pp. 1417–1434, 1986.

[9] A. Moody and A. Strahler, "Characteristics of composited AVHRR data and problems in their classification," *Int. J. Remote Sens.*, vol. 15, pp. 3473–3491, 1994.

[10] J.-L. Roujean, M. Leroy, A. Podaire, and P. Y. Deschamps, "Evidence of surface reflectance bidirectional effects from a NOAA/AVHRR multitemporal data set," *Int. J. Remote Sens.*, vol. 13, pp. 685–698, 1992.

[11] B. Meyer, M. M. Verstraete, and B. Pinty, "The effect of surface anisotropy and viewing geometry on the estimation of NDVI from AVHRR," *Remote Sens. Rev.*, vol. 12, pp. 3–27, 1995.

[12] W. van Leeuwen, B. J. Orr, S. E. Marsh, and S. M. Herrmann, "Multisensor NDVI data continuity: uncertainties and implications for vegetation monitoring applications," *Remote Sens. Environ.*, vol. 100, pp. 67–81, 2006.

[13] E. A. Walter-Shea, J. L. Privette, D. Cornell, M. A. Mesarch, and C. J. Hays, "Relations between directional spectral vegetation indices and leaf area and absorbed radiation in alfalfa," *Remote Sens. Environ.*, vol. 61, pp. 162–177, 1997.

[14] A. P. Trishchenko, J. Cihlar, and Z. Li, "Effects of spectral response function on surface reflectance and NDVI measured with moderate resolution satellite sensors," *Remote Sens. Environ.*, vol. 81, pp. 1–18, 2002.

[15] K. J. Linthicum, A. Anyamba, C. J. Tucker, P. W. Kelley, M. F. Myers, and C. J. Peters, "Climate and satellite indicators to forecast Rift Valley Fever epidemics in Kenya," *Science*, vol. 285, pp. 397–400, 1999.

[16] C. O. Justice, A. S. Belward, J. T. Morisette, P. Lewis, J. L. Privette, and F. Baret, "Developments in the 'validation' of satellite sensor products for the study of land surface," *Int. J. Remote Sens.*, vol. 21, pp. 3383–3390, 2000.

[17] J. T. Morisette, J. Nickeson, A. P. Santos, E. Vermote, and J. Pedelty, "Atmospherically corrected Landsat ETM+ imagery for the EOS land validation core sites," *Earth Observer*, vol. 16, pp. 15–17, 2004.

[18] C. J. Tucker, J. E. Pinzon, M. E. Brown, D. Slayback, E. W. Pak, R. Mahoney, E. Vermote, and N. El Saleous, "An extended AVHRR 8-km NDVI data set compatible with MODIS and SPOT vegetation NDVI data," *Int. J. Remote Sens.*, vol. 26, pp. 4485–4498, 2005.

[19] J. Pinzon, M. E. Brown, and C. J. Tucker, "Satellite time series correction of orbital drift artifacts using empirical mode decomposition," in *Hilbert-Huang Transform: Introduction and Applications*, N. Huang, Ed. Hackensack, NJ: World Scientific, 2005, pt. II, ch. 10.

[20] A. C. Pinheiro, J. L. Privette, R. Mahoney, and C. J. Tucker, "Directional effects in a daily AVHRR land surface temperature data set over Africa," *IEEE Trans. Geosci. Remote Sens.*, vol. 42, no. 9, pp. 1941–1954, Sep. 2004.

[21] A. Huete, K. Didan, T. Miura, E. P. Rodriguez, X. Gao, and L. G. Ferreira, "Overview of the radiometric and biophysical performance of the MODIS vegetation indices," *Remote Sens. Environ.*, vol. 83, pp. 195–213, 2002.

[22] *MODIS Documentation and Data Source*. Greenbelt, MD: NASA Goddard Space Flight Center, 2004.

[23] *Landsat 7 Data User's Handbook*. Greenbelt, MD: NASA Goddard Space Flight Center, 2004.
[24] E. F. Vermote, D. Tanre, J. L. Deuze, M. Herman, and J.-J. Morcrette, "Second simulation of the satellite signal in the solar spectrum, 6S: An overview," *IEEE Trans. Geosci. Remote Sens.*, vol. 35, no. 3, pp. 675–686, May 1997.
[25] B. N. Holben, T. F. Eck, I. Slutsker, D. Tanre, J. P. Buis, A. Setzer, E. Vermote, J. A. Reagan, Y. J. Kaufman, T. Nakajima, F. Lavenu, I. Jankowiak, and A. Smirnov, "AERONET—a federated instrument network and data archive for aerosol characterization," *Remote Sens. Environ.*, vol. 66, pp. 1–16, 1998.
[26] D. A. Quattrochi and M. F. Goodchild, *Scale in Remote Sensing and GIS*. Boca Raton, Florida: Lewis, 1999.
[27] N. Zeng, J. D. Neelin, and W. K.-M. Lau, "Enhancement of interdecadal climate variability in the Sahel by vegetation interaction," *Science*, vol. 286, pp. 1537–1540, 1999.
[28] L. Bounoua, G. J. Collatz, S. O. Los, P. J. Sellers, D. A. Dazlich, C. J. Tucker, and D. A. Randall, "Sensitivity of climate to changes in NDVI," *J. Clim.*, vol. 13, pp. 2277–2292, 2000.
[29] R. R. Nemani, C. D. Keeling, H. Hashimoto, W. M. Jolly, S. C. Piper, C. J. Tucker, R. B. Myneni, and S. W. Running, "Climate-driven increases in global terrestrial net primary production from 1982 to 1999," *Science*, vol. 300, pp. 1560–1563, 2003.
[30] S. W. Running, "Estimating terrestrial primary productivity by combining remote sensing and ecosystem simulation," in *Remote Sensing of Biosphere Functioning*, H. Mooney and R. Hobbs, Eds. New York: Springer-Verlag, 1990, pp. 65–86.
[31] "The International Geosphere-Biosphere Programme: A Study of Global Change, Improved Global Data for Land Applications," IGBP Secretariat, Stockholm, Sweden, IGPB Rep. No. 20, 1992.
[32] J. T. Morisette, J. L. Privette, and C. O. Justice, "A framework for the validation of MODIS land products," *Remote Sens. Environ.*, vol. 83, pp. 77–96, 2002.
[33] J. T. Morisette, J. E. Pinzon, M. E. Brown, C. J. Tucker, and C. O. Justice, "Initial validation of NDVI time series from AVHRR, vegetation and MODIS," in *Int. SPOT 4/5—VEGETATION Users Conf.*, Antwerp, Belgium, 2004.
[34] S. D. Prince, C. O. Justice, and S. O. Los, *Remote Sensing of the Sahelian Environment*. Brussels, Belgium: Technical Center for Agriculture and Rural Cooperation, 1990.
[35] M. Roderick, R. Smith, and S. Cridland, "The precision of the NDVI derived from AVHRR observations," *Remote Sens. Environ.*, vol. 56, pp. 57–65, 1996.
[36] G. Saint, "SPOT-4 vegetation system—association with high-resolution data for multiscale studies," *Adv. Space Res.*, vol. 17, pp. 107–110, 1995.
[37] C. O. Justice, E. Vermote, J. R. G. Townshend, R. Defries, D. P. Roy, D. K. Hall, V. V. Salomonson, J. L. Privette, G. Riggs, A. Strahler, W. Lucht, R. B. Myneni, Y. Knyazikhin, S. W. Running, R. R. Nemani, Z. M. Wan, A. R. Huete, W. van Leeuwen, R. E. Wolfe, L. Giglio, J. P. Muller, P. Lewis, and M. J. Barnsley, "The Moderate Resolution Imaging Spectroradiometer (MODIS): Land remote sensing for global change research," *IEEE Trans. Geosci. Remote Sens.*, vol. 36, no. 4, pp. 1228–1249, Jul. 1998.
[38] D. D. Baldocchi and K. B. Wilson, "Modeling CO2 and water vapor exchange of a temperate broadleaved forest across hourly to decadal time scales," *Ecolog. Model.*, vol. 142, pp. 155–184, 2001.
[39] A. Lawler, "Stormy forecast for climate science," *Science*, vol. 305, pp. 1094–1097, 2004.
[40] L. Ji and A. J. Peters, "Assessing vegetation response to drought in the northern great plains using vegetation and drought indices," *Remote Sens. Environ.*, vol. 87, pp. 85–98, 2003.
[41] J. Verdin, C. Funk, R. Kalver, and D. Roberts, "Exploring the correlation between southern Africa NDVI and Pacific sea surface temperatures: Results for the 1998 Maize growing season," *Int. J. Remote Sens.*, vol. 20, pp. 2117–2124, 1999.
[42] A. Anyamba, K. J. Linthicum, R. Mahoney, C. J. Tucker, and P. W. Kelley, "Mapping potential risk of Rift Valley Fever outbreaks in African savannas using vegetation time series data," *Photogramm. Eng. Remote Sens.*, vol. 68, pp. 137–145, 2002.
[43] N. V. Shabanov, L. M. Zhou, Y. Knyazikhin, R. B. Myneni, and C. J. Tucker, "Analysis of interannual changes in northern vegetation activity observed in AVHRR data from 1981 to 1994," *IEEE Trans. Geosci. Remote Sens.*, vol. 40, no. 1, pp. 115–130, Jan. 2002.
[44] D. A. Slayback, J. E. Pinzon, S. O. Los, and C. J. Tucker, "Northern hemisphere photosynthetic trends 1982–99," *Global Change Biol.*, vol. 9, pp. 1–15, 2003.
[45] J. A. Hicke, G. P. Asner, J. T. Randerson, C. Tucker, S. Los, R. Birdsey, J. C. Jenkins, and C. Field, "Trends in North American net primary productivity derived from satellite observations, 1982–1998," *Global Biogeochem. Cycles*, vol. 16, 10.1029/2001GB001550, 2002.

Molly E. Brown received the B.S. degree in biology and environmental studies from Tufts University, Medford, MA, in 1991, and the M.A. and Ph.D. degrees in geography from the University of Maryland, College Park, in 1998 and 2002, respectively.

She is currently a Research Scientist with the Biospheric Sciences Branch, NASA/Goddard Space Flight Center, Greenbelt, MD. She spent three years in West Africa in the U.S. Peace Corps. Her current research interests include vegetation monitoring in semi-arid regions, interdisciplinary research that joins socio-economic and remotely sensed biophysical data, and improving systems that use vegetation indices to give early warning of food insecurity and disease outbreak in developing countries.

Jorge E. Pinzón received the B.Sc. degrees in mathematics and computer science, respectively, from the Universidad de los Andes, Bogotá, Colombia, in 1985 and 1986, respectively, and the M.S. and Ph.D. degrees in applied mathematics from the University of California, Davis, in 1996 and 1998, respectively.

He was a Postdoctoral Fellow with the University of Maryland, College Park, for two years, and is currently with Science Systems and Applications, Inc. (SSAI), Biospheric Sciences Branch, NASA/Goddard Space Flight Center, Greenbelt, MD, as a Senior Scientist. His research interests include data representation and pattern recognition in time series and remote sensing.

Kamel Didan received the Ph.D. degree in agricultural and biosystem engineering with a minor in industrial engineering from the University of Arizona, Tucson, in 1999.

He is currently a Research Scientist with the Terrestrial Biophysics and Remote Sensing Laboratory, University of Arizona. He is a MODIS Associate Science Team Member and leads the research and development of the MODIS Vegetation Index algorithm and the surface reflectance-spatial aggregation algorithm. His research interests include the development of algorithms and models for calibrated time series analysis aimed at assessing climate-related and land use change influences on vegetation health and dynamics over different biomes. This research attempts to isolate the vegetation signal for biophysical and global change studies with satellite-based sensors.

Jeffrey T. Morisette received the B.A. degree from Siena Heights University, Adrian, MI, the M.S. degree in statistics from Oakland University, Rochester, MI, and the Ph.D. degree from North Carolina State University, Raleigh, where he focused on geostatistics, accuracy assessment, and satellite-based changed detection, funded through a NASA Earth System Science Graduate fellowship. He also attended the International Space University's Summer Program, Vienna, Austria, in 1996.

He is currently with the NASA Goddard Space Flight Center (GSFC), Greenbelt, MD. His current research is on the application of multiresolution satellite imagery to ecological studies and the validation of global land products with a focus on coordinating the MODIS land team validation activities through GSFC. He also works with the "Land Product Validation Subgroup" of the Committee on Earth Observing Satellite Working Group on Calibration and Validation helping to organize and coordinate international land product validation activities.

Compton J. Tucker received the B.S. degree in biology and the M.S. and Ph.D. degrees in forestry from Colorado State University, Fort Collins, in 1969, 1973, and 1975, respectively.

He is a Senior Fellow at the NASA/Goddard Space Flight Center, Greenbelt, MD, and has been with NASA since 1975. His research activities involve the use of satellite data to study tropical deforestation, desertification, ecologically coupled diseases, and terrestrial primary production. He founded and is the Head of the GIMMS Group in the Biospheric Sciences Branch.